Natural killer cells in the human lung tumor microenvironment display immune inhibitory functions

Jules Russick, Pierre-Emmanuel Joubert, Mélanie Gillard-Bocquet, Carine Torset, Maxime Meylan, Florent Petitprez, Marie-Agnes Dragon-Durey, Solenne Marmier, Aditi Varthaman, Nathalie Josseaume, et al.

▶ **To cite this version:**

Jules Russick, Pierre-Emmanuel Joubert, Mélanie Gillard-Bocquet, Carine Torset, Maxime Meylan, et al.. Natural killer cells in the human lung tumor microenvironment display immune inhibitory functions. Journal for Immunotherapy of Cancer, 2020, 8 (2), pp.e001054. 10.1136/jitc-2020-001054 . inserm-03975406

HAL Id: inserm-03975406
https://inserm.hal.science/inserm-03975406

Submitted on 6 Feb 2023

HAL is a multi-disciplinary open access archive for the deposit and dissemination of scientific research documents, whether they are published or not. The documents may come from teaching and research institutions in France or abroad, or from public or private research centers.

L'archive ouverte pluridisciplinaire **HAL**, est destinée au dépôt et à la diffusion de documents scientifiques de niveau recherche, publiés ou non, émanant des établissements d'enseignement et de recherche français ou étrangers, des laboratoires publics ou privés.

Journal for ImmunoTherapy of Cancer

Natural killer cells in the human lung tumor microenvironment display immune inhibitory functions

Jules Russick,[1] Pierre-Emmanuel Joubert,[1] Mélanie Gillard-Bocquet,[1] Carine Torset,[1] Maxime Meylan,[1] Florent Petitprez,[2] Marie-Agnes Dragon-Durey,[1,3] Solenne Marmier,[1] Aditi Varthaman,[1] Nathalie Josseaume,[1] Claire Germain,[1] Jérémy Goc,[1] Marie-Caroline Dieu-Nosjean,[4] Pierre Validire,[5] Ludovic Fournel,[6] Laurence Zitvogel,[7,8] Gabriela Bindea,[9] Audrey Lupo,[1,6] Diane Damotte,[1,6] Marco Alifano,[1,6] Isabelle Cremer [1]

To cite: Russick J, Joubert P-E, Gillard-Bocquet M, *et al*. Natural killer cells in the human lung tumor microenvironment display immune inhibitory functions. *Journal for ImmunoTherapy of Cancer* 2020;**8**:e001054. doi:10.1136/jitc-2020-001054

► Additional material is published online only. To view please visit the journal online (http://dx.doi.org/10.1136/jitc-2020-001054).

JR and P-EJ are joint first authors.

Accepted 15 September 2020

Check for updates

© Author(s) (or their employer(s)) 2020. Re-use permitted under CC BY-NC. No commercial re-use. See rights and permissions. Published by BMJ.

For numbered affiliations see end of article.

Correspondence to
Professor Isabelle Cremer, Centre de Recherche des Cordeliers, Sorbonne Université, Université de Paris, Inserm UMR S1138, Paris 75006, France; isabelle.cremer@crc.jussieu.fr

ABSTRACT

Background Natural killer (NK) cells play a crucial role in tumor immunosurveillance through their cytotoxic effector functions and their capacity to interact with other immune cells to build a coordinated antitumor immune response. Emerging data reveal NK cell dysfunction within the tumor microenvironment (TME) through checkpoint inhibitory molecules associated with a regulatory phenotype.

Objective We aimed at analyzing the gene expression profile of intratumoral NK cells compared with non-tumorous NK cells, and to characterize their inhibitory function in the TME.

Methods NK cells were sorted from human lung tumor tissue and compared with non- tumoral distant lungs.

Results In the current study, we identify a unique gene signature of NK cell dysfunction in human non-small cell lung carcinoma (NSCLC). First, transcriptomic analysis reveals significant changes related to migratory pattern with a downregulation of sphingosine-1-phosphate receptor 1 (S1PR1) and CX3C chemokine receptor 1 (CX3CR1) and overexpression of C-X-C chemokine receptor type 5 (CXCR5) and C-X-C chemokine receptor type 6 (CXCR6). Second, cytotoxic T-lymphocyte-associated protein 4 (CTLA-4) and killer cell lectin like receptor (KLRC1) inhibitory molecules were increased in intratumoral NK cells, and CTLA-4 blockade could partially restore MHC class II level on dendritic cell (DC) that was impaired during the DCs/NK cell cross talk. Finally, NK cell density impacts the positive prognostic value of $CD8^+$ T cells in NSCLC.

Conclusions These findings demonstrate novel molecular cues associated with NK cell inhibitory functions in NSCLC.

BACKGROUND

Natural killer (NK) cells are innate lymphoid cells representing the first line of defense against infected or transformed cells. They are highly cytotoxic, express many activating and inhibitory receptors and secrete cytokines and chemokines including tumor necrosis factor α(TNF-α), interferon γ (IFN-γ), C-C motif chemokine ligand 3 (CCL3) and granulocyte–macrophage colony-stimulating factor (GM-CSF), allowing them to attract and interact with other immune cells.[1]

In the tumor context, NK cell activation is tightly regulated by their interaction with malignant cells expressing various levels of NK receptor ligands. The current dogma is that NK cells act early in the antitumor immune response by controlling tumor burden and stimulating adaptive T cell immune responses[2] thereby curbing cancer cell metastasis.[3] NK cells and T cells cooperate to restrain tumor growth, highlighting a role for NK cells in shaping adaptive anticancer responses. Indeed, patients with defective NK cell functions have been shown to have a higher incidence of cancers,[4] while decreased peripheral blood NK cell activity is linked to increased carcinoma incidence.[5]

Intratumoral NK cells display altered phenotype and functional impairment, relative to non-tumorous NK (Non-Tum-NK) cells in patients with lung cancer,[6 7] prostate cancer,[8] breast cancer,[9] hepatocellular carcinoma[10] and gastrointestinal stromal tumors.[11] NK dysfunction has been attributed to direct cross talk between tumor cells and NK cells, activated platelets and several soluble factors, such as myeloid derived suppressor cells, macrophage-derived and tumor cell-derived transforming growth factor β (TGF-β), prostaglandin E2, indoleamine-2,3-dioxygenase, adenosine and interleukin-10 (IL-10).[4 7] In addition, loss of antitumor effects in NK cells closely associated with aberrant fructose-1,6-biphosphatase-induced inhibition of glycolysis, and reduced NK cell viability.[12] This can be explained by persistent stimulatory signaling and/or evading strategies used by tumor cells to escape NK cells, including the

J Immunother Cancer: first published as 10.1136/jitc-2020-001054 on 16 October 2020. Downloaded from http://jitc.bmj.com/ on February 6, 2023 at INSERM Consortia. Protected by copyright.

downregulation of important NK cell-activating ligands and/or an immunosuppressive tumor microenvironment (TME).

In non-small cell lung carcinoma (NSCLC), whereas tumor infiltrating $CD8^+$ T cells, $CD20^+$ B cells and DC-$LAMP^+$ mature dendritic cells (DCs) strongly associate with a good clinical outcome,[13–15] NK cell density is not linked to a prognostic value.[7 16 17] This discrepancy can be explained by the fact that the TME is able to locally edit the phenotype of intratumoral NK cells, leading to reduced expression of activating receptors, increased expression of the inhibitory receptor natural killer group (NKG) 2A.[7 18] NK cells may also acquire other immune checkpoint molecules[19 20] such as programmed death-1 (PD-1), lymphocyte-activation gene 3, T cell immunoreceptor with Ig and ITIM domains (TIGIT), T cell immunoglobulin and mucin domain-containing protein 3 (TIM3), CD73[21] and cytokine-inducible SH2-containing protein[22] in certain tumor contexts. Preclinical studies show that NKG2A or TIGIT blockade enhances antitumor immunity mediated by NK cells,[23–25] demonstrating the importance of targeting NK cells.

Microarray analysis of intratumoral, as compared with distant lung tissue NK cells, reveal a specific transcriptional signature suggesting modulation of NK cell activity within the TME.[26] However, the significance of this tumor-induced signature has not been investigated so far. Here, we demonstrate, for the first time, that human NK cells express cytotoxic T-lymphocyte-associated protein 4 (CTLA4) in the lung, which is upregulated within the TME, and have a distinct expression of migratory receptors. Our data also show that CTLA4-expressing NK cells have a negative impact on DCs within the TME and impact the overall survival (OS) of $CD8^+$T cells in patients with NSCLC.

MATERIAL AND METHODS

Tissue samples from patients with NSCLC

Human primary NSCLC samples and non-tumorous distant tissues (situated at more than 10 cm from the tumor) were obtained from non-treated patients the day of surgery at Institut Mutualiste Montsouris (Paris), Hotel-Dieu Hospital (Paris) or Cochin Hospital (Paris), from two prospective studies (see online supplementary tables 1 and 4, respectively, cohort 1 discovery cohort and cohort 2 validation cohort). A retrospective NSCLC cohort was also used in this study (cohort 3). Cohort 3 includes 539 untreated patients seen between 2001 and 2005 at the Department of Thoracic Surgery of Hotel-Dieu Hospital (Paris, France).[27] The inclusion criteria are histological subtypes squamous cell carcinoma (SCC) or lung adenocarcinoma (ADC), all TNM stages classification and associated with clinical data. Histopathologic features such as histological subtypes, ADC grade and TNM stages are available for the majority of the patients.

Preparation of human single-cell suspension

Surgical samples were mechanically dilacerated and single-cell suspensions obtained after non-enzymatic disruption using the Cell Recovery Solution (Corning) for 1 hour at 4°C under agitation and filtered through a 70 µm cell strainer (BD Biosciences). Cells were washed in phosphate-buffered saline (PBS)+5% foetal calf serum (FCS)+ ethylenediaminetetraacetique (EDTA) 0.5 mM and mononuclear cells were purified using Lymphocyte Separation Medium gradient (Eurobio, Les Ulis, France). The number of cells obtained was then determined by manual counting on Kova slides (Kova International, Garden Grove, California, USA) for further use.

NK cell sorting

Mononuclear cells were incubated with Live/Dead Fixable Yellow Dead Cell Stain Kit (ThermoFischer, Waltham, Massachusetts, USA), phycoerythrin (PE)-conjugated anti-CD45 (mIgG1κ, clone J.33, Beckman Coulter), Fluorescein isothiocyanate (FITC)-conjugated anti-CD3 (BioLegend San Diego, California, USA. mIgG1κ, clone UCHT1), allophycocyanin (APC)-conjugated anti-CD56 (BD Biosciences, Allschwil, Suisse, mIgG2bκ, clone N-CAM16.2) and alexafluor (AF)700-conjugated anti-CD11c (BD Biosciences, mIgG1κ, clone B-ly6) for 30 min at 4°C and sorted with an fluorescence activated cell sorting (FACS) Aria III cell sorter (BD Biosciences). Sorted NK cells were defined as $CD45^+CD3^-CD56^+$ cells, DC as $CD11c^+$ cells and purity after sorting was validated by flow cytometry data using Diva software (BD Biosciences). For RNA analysis, sorted NK cells were immediately collected in lysis buffer supplied in the RNA extraction kit (RNeasy Microkit—Qiagen, Maryland, USA).

Flow cytometry

Cells were counted and stained using Live/Dead Fixable Yellow Dead Cell Stain Kit, CD45-PE or FITC (Clone HI30, BioLegend), CD3-FITC (Clone UCHT1, ThermoFisher) or PerCP-Cy5.5 (Clone SK7, BioLegend), CD56-APC or BV421 (Clone HCD56, BioLegend), NKp46-BV650 (9E2, BD Biosciences), CX3C chemokine receptor 1 (CX3CR1)-APC (Clone 2A9-1, ThermoFisher), CD107a-APC-H7 (H4A3, BD Biosciences), killer cell lectin like receptor C1 (KLRC1)-PE (Z199, Beckman Coulter), EOMES-PE eFluor610 (Clone WD1928, ThermoFisher), C-X-C chemokine receptor type 6 (CXCR6)-Pe-Cy7 (Clone SA051D1, BioLegend), BV450-conjugated anti-FoxP3 (Clone 259D/C7, BD Biosciences, mIgG1) and BV786-conjugated anti-CTLA4 (Clone BNI3, BD Biosciences, mIgG2aκ).

Antibodies and cells were incubated in PBS, 10% FCS, 0.5 mM EDTA medium for 30 min at 4°C and washed. Staining was acquired on Fortessa X20 (BD Biosciences) and analyzed using FlowJo software.

Microarray experiment and analysis

Microarray analysis was performed from previously described experiment.[26]

J Immunother Cancer: first published as 10.1136/jitc-2020-001054 on 16 October 2020. Downloaded from http://jitc.bmj.com/ on February 6, 2023 at INSERM Consortia. Protected by copyright.

RNA extraction from NK cells

Total RNA was extracted with the RNEasy Micro Kit (Qiagen) according to the manufacturer's instructions. RNA quality and quantity were analyzed on a PicoChip (Total Eukaryote RNA Assay Pico II Kit; Qiagen) by capillary electrophoresis (BioAnalyzer; Agilent).

Reverse transcription and preamplification

Reverse transcriptions were performed on 5 ng of total RNA in a 20 µL reaction volume with the High Capacity cDNA Reverse Transcription Kit with RNAse inhibitor (PN 4368814; AppliedBiosystems) according to the manufacturer's instructions.

Overall, 12.5 µL of cDNAs were preamplified with the Taqman Preamp Master Mix Kit (AppliedBiosystems) in a 50 µL reaction volume containing 25 µL of Master Mix 2× and 12.5 µL of a pooled assay. Pooled assays combined equal volumes of each 20×Taqman Gene Expression Assay of interest including the endogenous gene *CDKN1B* diluted using 1×TE buffer so that each assay is at a final concentration of 0.2×. A 14 cycles preamplification was performed, as recommended by the manufacturer and preamplification products were 1:20 diluted in 1×TE buffer.

Semiquantitative real-time polymerase chain reaction (PCR)

Semiquantitative real-time PCR was performed with FastStart Universal Probe Master Mix (Rox) 2× with 20×Taqman Gene Expression Assay and 6.25 µL of preamplified cDNA in a 25 µL total reaction volume in each well of a 96-well plate. CDKN1B endogenous gene was used as recommended by the manufacturer in the PreAmp Master Mix Protocol. 7900HT Fast Real-Time PCR System (AppliedBiosystems) was used for the detection and semiquantification of gene expression.

TaqMan Array Micro Fluidic Cards (Low-Density Arrays 384-wells format) were customized with our genes of interest and performed with FastStart Universal Probe Master Mix (Rox) 2× and preamplified cDNA in a 100 µL total reaction volume on the 7900HT Fast Real-Time PCR System (AppliedBiosystems).

Quantitative real-time PCR results were analyzed with the dedicated SDS V.2.3 and RQManager softwares (AppliedBiosystems). For each probe and each sample, we normalized gene expression with the CDKN1B endogenous gene expression (ΔCt) and calculated the ΔΔCt and the corresponding fold change ($2^{-\Delta\Delta Ct}$) between the tumorous NK (Tum-NK) and the Non-Tum-NK samples for each patient.

Immunohistochemistry

Tissues were deparaffinized and rehydrated by successive baths of Clearene and ethanol gradient (100%, 90%, 70% and 50%). Antigen retrieval was performed with a Tris-EDTA pH8 solution in a preheated water bath (97°C, 30 min). Sections were cooled at room temperature for 30 min and endogenous peroxidase was blocked with 3% hydrogen peroxide (15 min). Thereafter, sections were incubated with Protein Bock solution (Dako) for 30 min and incubated with mouse anti-human NKp46 (clone 195314, R&D Systems, 5 µg/mL) and/or goat anti-human CTLA4 mAb (AF-386-PB, R&D Systems, 2.5 µg/mL) for 1 hour at room temperature. Peroxidase-linked secondary antibody (ImmPress anti-goat HRP Vector) and alkaline phosphatase-linked secondary antibody (Rabbit anti-mouse AP Rockland Immunochemicals) were used for CTLA4 and NKp46, respectively. 3-Amino-9-ethylcarbazole and shrimp alkaline phosphatase substrate (Vector laboratories) were used to detect specific staining. For immunofluorescence detection, PE-conjugated donkey anti-goat (Jackson ImmunoResearch) and AF647-conjugated donkey anti-mouse (Jackson ImmunoResearch) 1:100 diluted were used for CTLA4 and NKp46, respectively. Mounting medium containing 4',6-diamidino-2-phénylindole (DAPI) was used (Prolong Gold Antifade Mountant with DAPI, Invitrogen). Immunofluorescence was detected with AxioVert 200 microscope (Zeiss).

NKp46 quantification and image quantification (cohort 3)

NKp46 was stained by immunohistochemistry for 309 patients of the retrospective cohort (cohort 3). Slides were then digitalized using a NanoZoomer scanner (Hamamatsu Photonics, Hamamatsu, Japan) and NKp46 density was quantified (NK cell number per mm^2 tumorous tissue) with Calopix software (Tribune Healthcare, France).

CD8 staining of NSCLC validation cohort (cohort 2) and image quantification

Serial 5 µm formalin-fixed paraffin-embedded NSCLC sections were stained using the Dako Autostainer Plus. Heat-mediated antigen retrieval was performed using the EnVision FLEX Target Retrieval Solutions (Agilent, Dako, California, USA) at pH9 for 30 min on a PT-Link (Dako). Immunodetection of CD8 expression was done using a mouse anti-human CD8 antibody (Clone C8/144B). (Dako) at 1.6 µg/mL for 30 min in Dako REAL Antibody Diluent (Dako). Signal intensity was improved with EnVision +System-HRP-labeled Polymers anti-mouse (Dako) and peroxidase was detected using diaminobenzidine +Substrate—Chromogen System (Dako). Slides were then counterstained with Hematoxylin (Dako) and mounted with Glycergel Mounting Medium (Dako). Slides were then digitalized using a NanoZoomer scanner (Hamamatsu Photonics, Hamamatsu, Japan) and CD8 density was quantified with Halo software (Indica Labs, New Mexico, USA).

CD107a degranulation assay

Tumor infiltrating lymphocytes (TILs) from patients with NSCLC were cultured for 12 hours in the presence of 100 U/mL IL-2 and incubated with K562 or P815 target cells at effector–target ratios of 10:1 during 4 hour, in the presence or not of anti-CD16 Ab, with monensin and PE Cy5-conjugated anti-CD107a (LAMP-1) mAb. Cells were

J Immunother Cancer: first published as 10.1136/jitc-2020-001054 on 16 October 2020. Downloaded from http://jitc.bmj.com/ on February 6, 2023 at INSERM Consortia. Protected by copyright.

then washed in PBS–FCS–EDTA and stained for 20 min at 4°C with FITC-conjugated anti-CD3 and APC-conjugated anti-CD56 or control conjugated isotypes.

Co-cultures of dendritic and NK cells

Tumor samples were processed as previously described (see 'preparation of human single-cell suspension'). NK cells and DC cells were sorted using Singlet/Live/CD45$^+$/CD3$^-$/CD56$^+$ and Singlet/Live/CD45$^+$/CD11c$^+$, respectively. Purity after cell isolation. The purity of cell subsets after cell sorting was assessed via flow cytometry prior to co-cultures and was between 94.6% and 100%, and between 98% and 99.6%, for NK cells and DCs, respectively. Cells were then plated in a 96-well U bottom plate (30–50×10^3 cells/well) in RPMI 1640 GlutaMAX (ThermoFisher) supplemented with human serum (Sigma-Aldrich, St-Louis, Missouri, USA) and penicillin–streptomycin (ThermoFisher) at 1:1 ratio of DC:NK. In the corresponding conditions, lipopolysaccharide (LPS-EB—InVivoGen, San Diego, California, USA) and blocking anti-CTLA4 antibody (ThermoFisher; clone AS32) were added at 1 µg/mL and at 5 µg/mL, respectively. DC activation was assessed after 48 or 72 hours of co-culture by flow cytometry. Cells were stained using an APC Cy7-conjugated anti-HLA-DR (mIgG2aκ, clone L243, BioLegend) and an AF700-conjugated anti-CD86 (mIgG1κ, clone 2331, BD).

CTLA4 and cytokine quantification produced by NK cells

Cell suspension from tumorous or non-tumorous tissues were obtained as described in 'preparation of human single-cell suspension'. The cells were incubated overnight in a 96-well plate in RPMI 1640 GlutaMAX supplemented with 10% human serum and 1% penicillin–streptomycin, then the supernatant was kept at −80°C for CTLA4 and cytokine dosages. Soluble CTLA4 was quantified using the ELISA Kit (Abcam) in the supernatant of cell cultures, following the manufacturer's protocol. Cytokine production in the supernatant of cell cultures was evaluated using Luminex Assay (Bio-Plex Pro Human Cytokine 27-plex Assay—BioRad), following the manufacturer's protocol.

Statistical and data analyses

Statistical analysis was performed using the R software V.3.6.0 and the packages pheatmap and ggplot2. Gene enrichment analysis was achieved with ClueGO[28] app of Cytoscape[29] with the Gene Ontology (GO) Biological processes database 2016 December. Association between quantitative and qualitative variables was estimated with Mann-Whitney U test. Association between quantitative variables was assessed using Pearson's correlation. Association between qualitative variables was assessed using Fisher's test. A p value <0.05 was considered statistically significant. The OS curves of patients with low-versus-high (separated by median) density of NKp46$^+$, CD8$^+$ T, DC-LAMP$^+$ DC or CD20$^+$ B cells, cells were estimated by the Kaplan-Meier method and compared by the log-rank test and was performed using the script 'survfit' on R studio software.

RESULTS

NK cells in the TME display a distinct transcriptomic signature

To determine whether the gene expression signature of intratumoral NK cells is distinct in the lung TME, a whole transcriptome analysis was previously performed on purified NK cells from the tumor and matched distant tissue, in a discovery cohort of 12 patients with NSCLC (see online supplemental table S1).[26] In the present study, we performed a more extensive analysis of microarray data, and found a total of 968 genes differentially expressed between intratumoral NK cells and Non-Tum-NK cells, with 569 overexpressed and 399 underexpressed genes, using the log2 fold change threshold of 1, with a p value inferior to 0.05 (figure 1A) demonstrating that NK cells in the TME have a distinct transcriptomic signature. Figure 1B illustrates expression levels of these upregulated and downregulated genes.

A GO analysis using Cluego revealed that differentially expressed genes were involved in cell migration, regulation of response to stimulus, cell activation, defense response and inflammatory response (figure 1C), supporting major functional changes of NK cells within the TME. The underexpressed genes were associated with inflammatory response, endocytosis, response to inorganic substance, blood coagulation and hemostasis, whereas the overexpressed ones were mainly associated with regulation of cell proliferation, cell activation and migration (figure 1D). Among the complete list of the 968 most differentially expressed genes (see online supplemental tables S2 and S3), those strongly linked to NK cell functions in the TME, that is, migration, cell activation and regulation of immune responses and cytotoxicity, were selected to analyze their expression in a validation cohort of 47 patients with NSCLC (see online supplemental table S4).

The selected gene signature included sphingosine-1-phosphate receptor 1 (S1PR1), CX3CR1, C-X-C chemokine receptor type 5 (CXCR5), CXCR6 and C-X-C motif ligand 13 (CXCL13) (figure 2A), cytotoxic T-lymphocyte-associated protein 4 (CTLA4), Fc receptor-like protein 4 (FCRL4), interleukin 22 receptor subunit alpha 2 (IL22RA2) and leukocyte immunoglobulin-like receptor pseudogene 2 (LILRP2) (figure 2B) and FS7-associated cell surface antigen (FAS), granzyme A-encoding gene (GZMA), granzyme K-encoding gene (GZMK), natural cytotoxicity triggering receptor 2 (NCR2) and KLRC1 (figure 2C). Semiquantitative qRT-PCR analysis performed on NK cells purified from tumor and matched non-tumor samples of the validation cohort confirmed the significant downregulation of S1PR1 and CX3CR1, and the overexpression of CXCR5, CXCR6, CXCL13, CTLA4, FCRL4, IL22RA2, LILRP2, FAS, GZMA, GZMK, NCR2 and KLRC1 (figure 2A–C). Unsupervised hierarchical clustering of samples based on this gene

J Immunother Cancer: first published as 10.1136/jitc-2020-001054 on 16 October 2020. Downloaded from http://jitc.bmj.com/ on February 6, 2023 at INSERM Consortia. Protected by copyright.

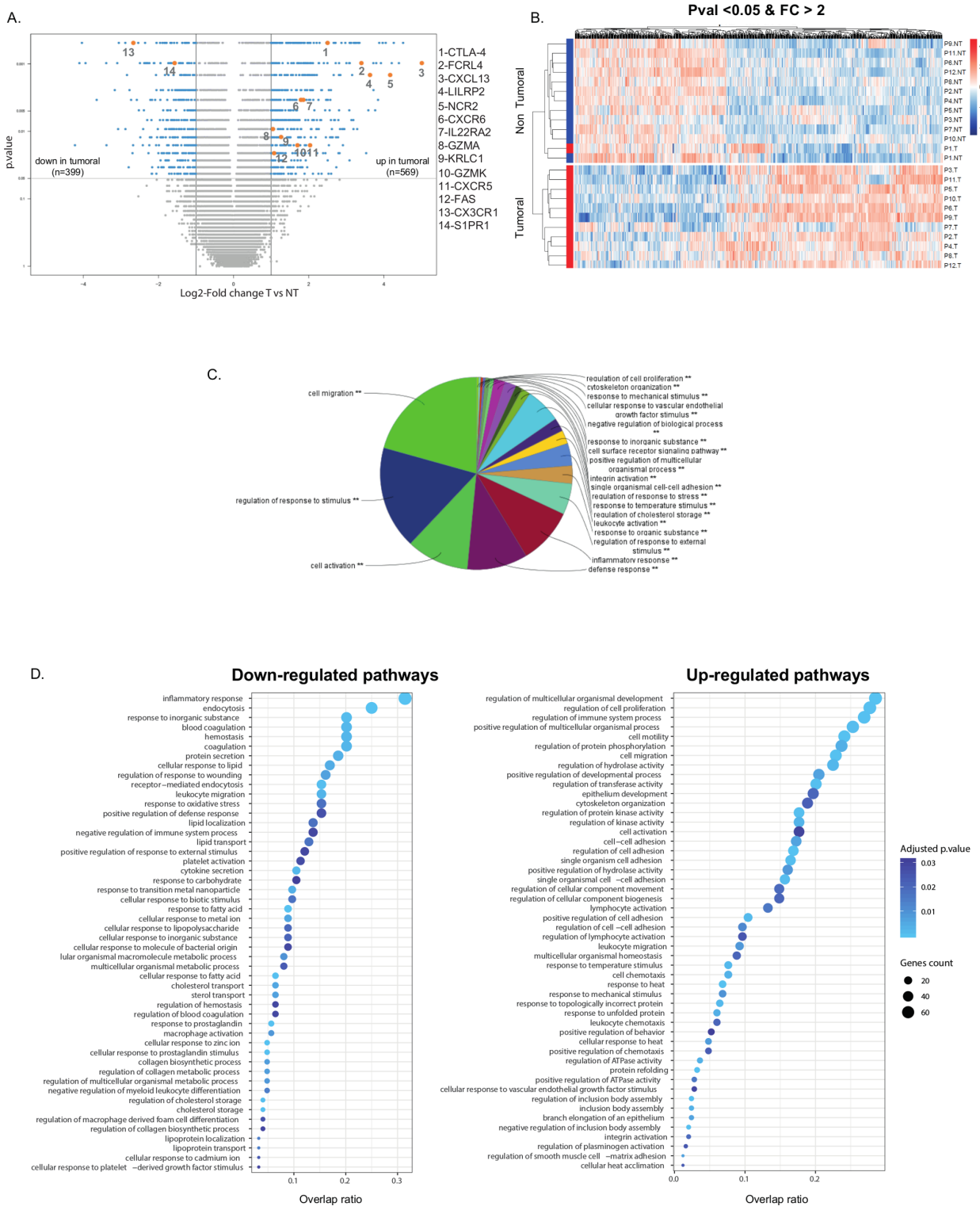

Figure 1 Gene expression differential analysis of tumorous versus non-tumorous (T vs NT) natural killer (NK) cells, in the discovery cohort (cohort 1). (A) Volcano plot presenting differentially expressed genes between tumorous NK and non-tumorous NK cells. X-axis displays log2 fold changes (FC) between the two groups and Y-axis the $-\log_{10}$(p value). Differentially expressed genes (highlighted in cyan) between tumorous and non-tumorous samples were characterized by fold changes superior/inferior to two and with a significant p value (<0.05). Genes of interest are colored in orange. (B) Heatmap of differentially expressed genes between tumorous and non-tumorous groups, organized by hierarchical clustering (after normalization of expression values). (C) Gene enrichment analysis for all the differentially expressed genes, using ClueGo application (Cytoscape software), with a significant p value (**). (D) Gene enrichment analysis for downregulated (left panel) and upregulated (right panel) biological processes. Color intensity of dots is proportional to the adjusted p values and size corresponds to the number of differentially expressed genes in the discovery cohort. Horizontal axis represents overlap between differentially expressed genes and genes in the biological processes.

J Immunother Cancer: first published as 10.1136/jitc-2020-001054 on 16 October 2020. Downloaded from http://jitc.bmj.com/ on February 6, 2023 at INSERM Consortia. Protected by copyright.

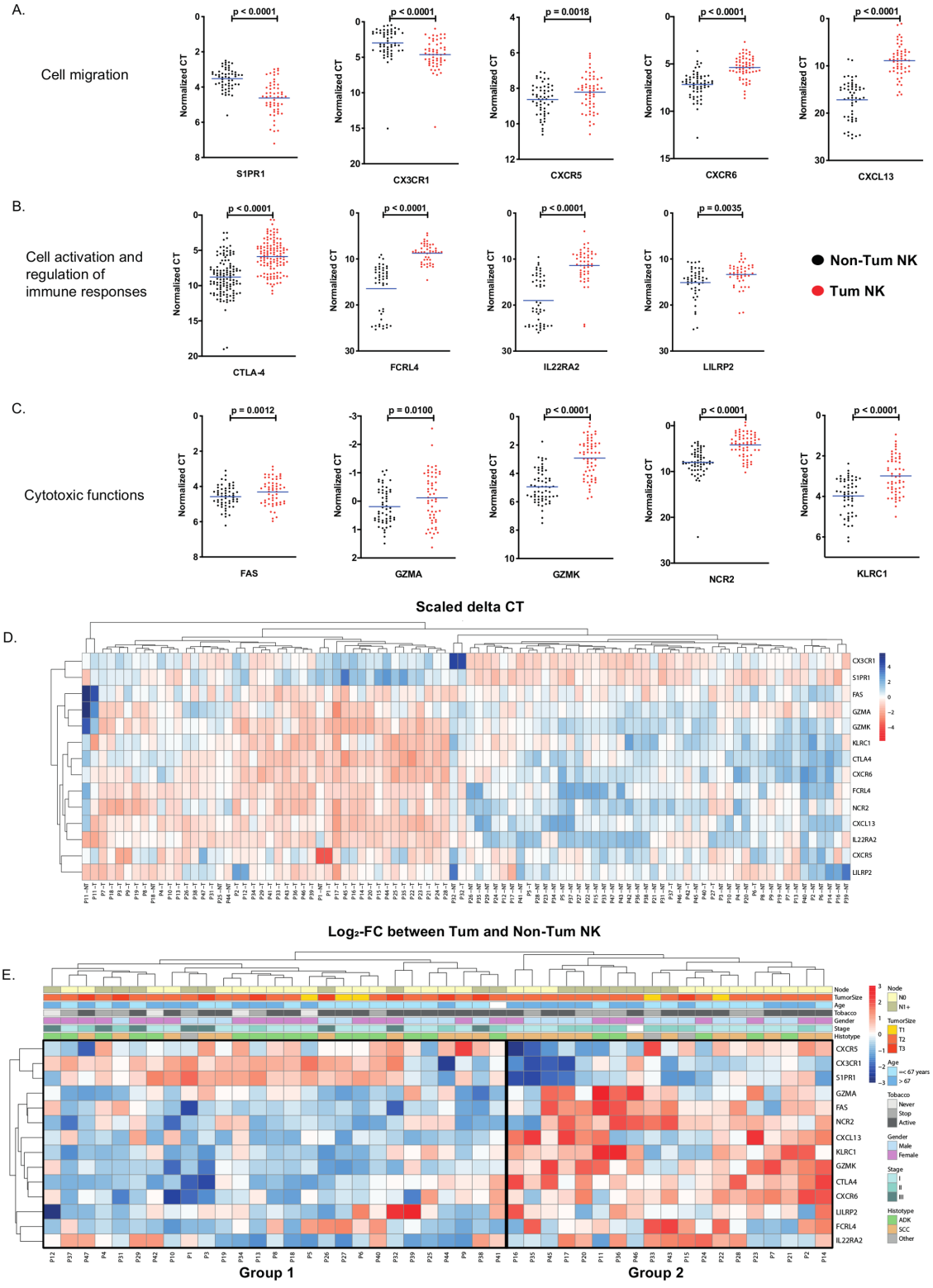

Figure 2 Specific gene variation between tumorous versus non-tumorous natural killer (NK) cells in the validation cohort (cohort 2) NK cells were sorted from non-tumorous distant tissue (Non-Tum NK—black dots) and from tumor (Tum NK—red dots) for 47 patients and total RNA were extracted and analyzed for the expression of 14 genes involved in NK migration (A), cell activation and regulation of immune responses (B) and cytotoxic functions (C) by quantitative PCR. Each dot represents a duplicate measurement of the gene expression in one individual. The mean values are indicated by blue dashes. Statistical differences were assessed by the Wilcoxon non-parametric test method with GraphPad software. (D) Heatmap of ΔΔCT for tumorous and non-tumorous samples of the 14 genes of interest. Hierarchical clustering identified two groups. Expression values were standardized. (E) Heatmap of fold changes of ΔΔCT values between tumorous and non-tumorous for the 14 genes of interest. Patient information are represented on top for each sample. FC, fold change; ADK, adenocarcinoma; SCC, squamous cell carcinoma.

J Immunother Cancer: first published as 10.1136/jitc-2020-001054 on 16 October 2020. Downloaded from http://jitc.bmj.com/ on February 6, 2023 at INSERM Consortia. Protected by copyright.

expression signature resulted in segregation of Tum-NK and Non-Tum-NK cells into distinct groups (figure 2D), confirming the modulation of NK cell migration, activation and cytotoxic functions in the TME. Unsupervised clustering based on expression variation of these genes in tumor NK cells compared with non-tumor NK cells revealed two groups of patients (figure 2E), with and an enrichment in migratory capacities in group 1 and in cytotoxic molecules in group 2. The two groups did not differ based on gender, tobacco, age, tumor size or presence of invaded lymph nodes (see online supplemental figure S1). However, we could notice an enrichment in stage 1 and 2 tumors and a trend for SCC histologic type enrichment in group 2 (see online supplemental figure S1).

A subset of intratumoral NK cells express CTLA4

Although CTLA4 is mainly expressed on regulatory T cells (Tregs) and some activated conventional T cell subsets (Tconv)[30] our analysis showed a strong upregulation of CTLA4 mRNA in intratumoral NK cells in a subset of patients (77 %) (figure 2B). This expression was then validated at the protein level by immunohistochemistry and flow cytometry analyses. We observed the co-expression of CTLA4 and NKp46 on intratumoral NK cells by immunohistochemistry and immunofluorescence on lung tumor tissue sections (figure 3A,B). Of note, the expression of CTLA4 by intratumoral NK cells was also observed in other solid tumors including melanoma, breast cancer and renal cell carcinoma (see online supplemental figure S2).

CTLA4 expression was then compared by flow cytometry in NK, Tconv and Treg cells in several patients (figure 3C). CTLA4 expression in Tregs within the tumor as well as in distant lung non-tumorous tissue was confirmed both at the cell surface and intracellularly, whereas CTLA4 was only expressed intracellularly by a fraction of NK and Tconv (figure 3D). In line with the results obtained by quantitative PCR, intracellular CTLA4 was highly overexpressed in intratumoral NK cells in 11 out of 16 patients tested (69%) (figure 3D). We, therefore, compared clinical data and survival of groups of patients with high and low CTLA4$^+$ NK cells and found that there are significantly more patients with low CTLA4$^+$ NK cells with ADC histological type (75% vs 32%, p=0.02) and having stage I NSCLC (75% vs 40%, p=0.07). We also found an influence of the gender since more female are found in the group of low CTLA4$^+$ NK cells patients (81% vs 42%, p=0.01). Other clinical parameters were similar between patients with high and low CTLA4$^+$ NK cells (see online supplemental figure S3A). We also found no difference in the OS between the two groups of patients (see online supplemental figure S3B).

NK cells in the TME have a distinct phenotype and cytokine secretion profile

To better characterize the NK cells in the TME, we performed a flow cytometry analysis and quantified cytokine production by sorted NK cells. We first observed that among CD3$^-$CD56$^+$ NK cells, most of NKp46$^+$ cells co-express the transcription factor Eomes, which confirms that the cells belong to the NK lineage (figure 4A,B). We found a significant higher expression of NK2GA and CXCR6 and lower expression of CX3CR1 in NK cells from the TME as compared with NK cells from non-tumorous tissue, confirming at the protein level the results obtained with gene expression analyses (figure 4A). Interestingly, we found that intratumoral NK cells display an activated phenotype, with high expression of CD69 and NKp44. However, no difference was found for FAS, CD107a and Eomes when we compared NK cells from TME or adjacent tissue (figure 4A). We also confirmed the co-expression of CTLA4 and NKp46 by NK cells, and the co-expression of inhibitory CTLA4 and NKG2A molecules on a subset of NK cells (figure 4B).

We found that NK cells from TME produced various levels of cytokines, with high levels of IL-1β, IL1RA, IL-6, IL-8, IL-9, IL-15, IL-17, TNF-α, IFN-γ and GM-CSF and in similar amounts compared with NK cells from adjacent tissue (figure 4C).

Intratumoral NK cells has reduced cytotoxicity and negatively regulate DC maturation

We had previously demonstrated that intratumoral NK had reduced capacity to degranulate and to secrete IFN-γ after a co-culture with autologous tumor cells.[7] We also show that NK cells display reduced cytolytic function in a redirected lysis assay, against P815 mastocytoma cells (see online supplemental figure S4).

To analyze a possible regulatory role of intratumoral NK cells, we co-cultured purified NK cells (CD3$^-$CD56$^+$) from fresh lung tumors and CD11c$^+$ DCs purified from the blood of the same patients in the presence of LPS stimuli. When NK cell numbers permitted, we analyzed DC maturation in the presence of a blocking anti-CTLA4 monoclonal antibody (mAb). After two to 2–3 days of co-culture, DC maturation was assessed by flow cytometry (figure 5A, and gating strategy online supplementary figure S5). Induction of major histocompatibility complex (MHC) class II and CD86 expression on DCs was significantly reduced on co-culture with intratumoral NK cells (20% and 41% inhibition, respectively) (figure 5B), and this was partially reverted by the addition of anti-CTLA4 mAb (figure 5C). In addition, we did not find any CTLA4 protein in the supernatant of intratumoral NK cells (data not shown). These data suggest that intratumoral NK can reduce DC activation, through a mechanism that partially involves CTLA4.

CTLA4 expression by intratumoral NK cells is highly correlated with CXCR6, GZMK and KLRC1

To understand the suppressive effect of intratumoral NK cells on DC maturation, we evaluated the correlations between the expression of CTLA4 and other genes in the signature. In tumors, we found an inverse correlation with S1PR1, and a strong positive correlation with

J Immunother Cancer: first published as 10.1136/jitc-2020-001054 on 16 October 2020. Downloaded from http://jitc.bmj.com/ on February 6, 2023 at INSERM Consortia. Protected by copyright.

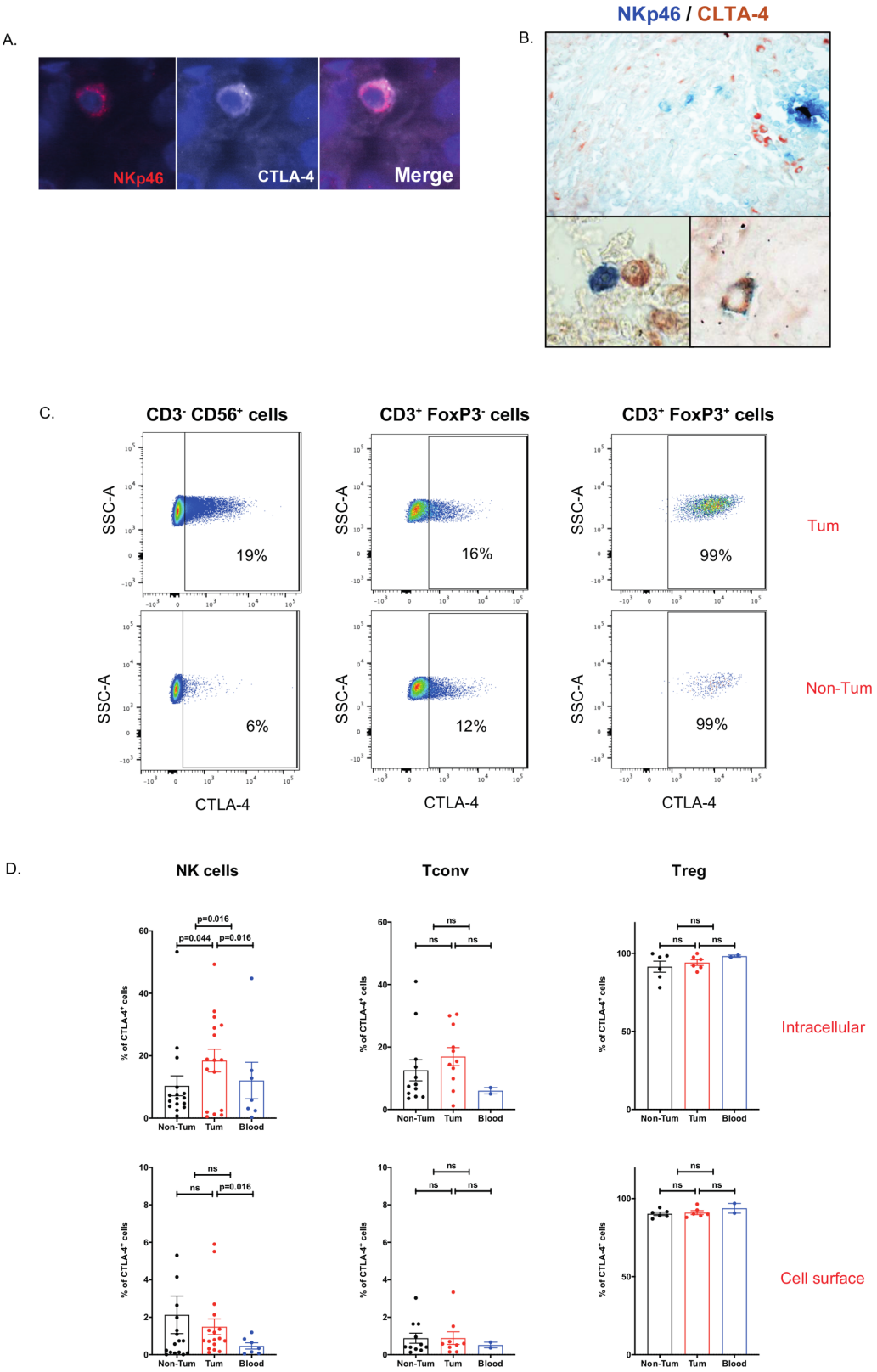

Figure 3 Cytotoxic T-lymphocyte-associated protein 4 (CTLA4) protein expression in tumor infiltrating natural killer (NK) cells. (A,B) Identification of CTLA4-expressing NKp46$^+$ cells in patients with non-small cell lung carcinoma (NSCLC) by immunofluorescence (A) or immunohistochemistry (B) double staining. (C,D) CTLA4 protein expression was analyzed in NK cells (CD3$^-$ CD56$^+$), conventional T cells (Tconv) (CD3$^+$ CD56$^-$ Foxp3$^-$) and regulatory T cells (Tregs) (CD3$^+$ CD56$^-$ Foxp3$^+$) by flow cytometry after intracellular or cell surface staining of cells from tumorous (Tum) or non-tumorous (Non-Tum) tissue of patients with NSCLC. Cells from blood were also analyzed for some patients. Representative images of intracellular CTLA4 staining are shown in (C) and the summary of analyzes are shown in (D). Statistical analyses were performed by Wilcoxon method with the GraphPad software. ns: not significant.

J Immunother Cancer: first published as 10.1136/jitc-2020-001054 on 16 October 2020. Downloaded from http://jitc.bmj.com/ on February 6, 2023 at INSERM Consortia. Protected by copyright.

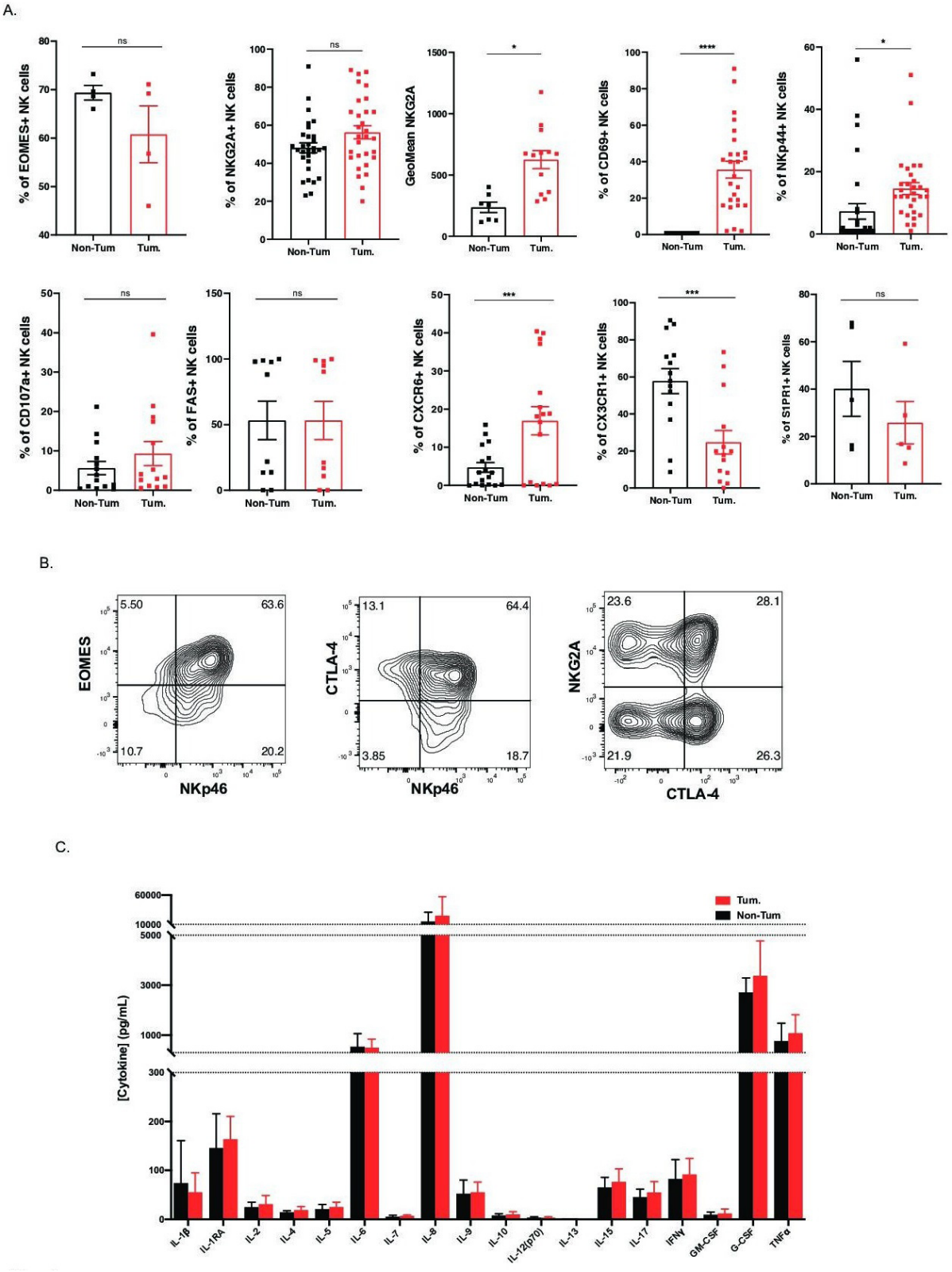

Figure 4 Intratumoral NK cells phenotype and cytokine secretion. (A) Eomes, NKG2A, CD69, NKp44, CD107a, FS7-associated cell surface antigen (FAS), C-X-C chemokine receptor type 6 (CXCR6), CX3CR1 and sphingosine-1-phosphate receptor 1 (S1PR1) protein expression were analyzed in natural killer (NK) cells ($CD3^{-}CD56^{+}$) by flow cytometry after cell surface staining of cells from non-tumorous (Non-Tum) or tumorous (Tum) tissue of patients with non-small cell lung carcinoma. Percentages or GeoMean is presented. (B) Co-staining for NKp46/Eomes, NKp46/cytotoxic T-lymphocyte-associated protein 4 (CTLA4) and CTLA4/NKG2A is shown on $CD3^{-}CD56^{+}$ intratumoral NK cells. (C) Quantification of cytokines produced by NK cells sorted from Tum or Non-Tum tissue. Statistical analyses were performed by Wilcoxon method with the GraphPad software. ns: not significant. *p<0.05; **p<0.01; ***p<0.001; p<0.0001.

J Immunother Cancer: first published as 10.1136/jitc-2020-001054 on 16 October 2020. Downloaded from http://jitc.bmj.com/ on February 6, 2023 at INSERM Consortia. Protected by copyright.

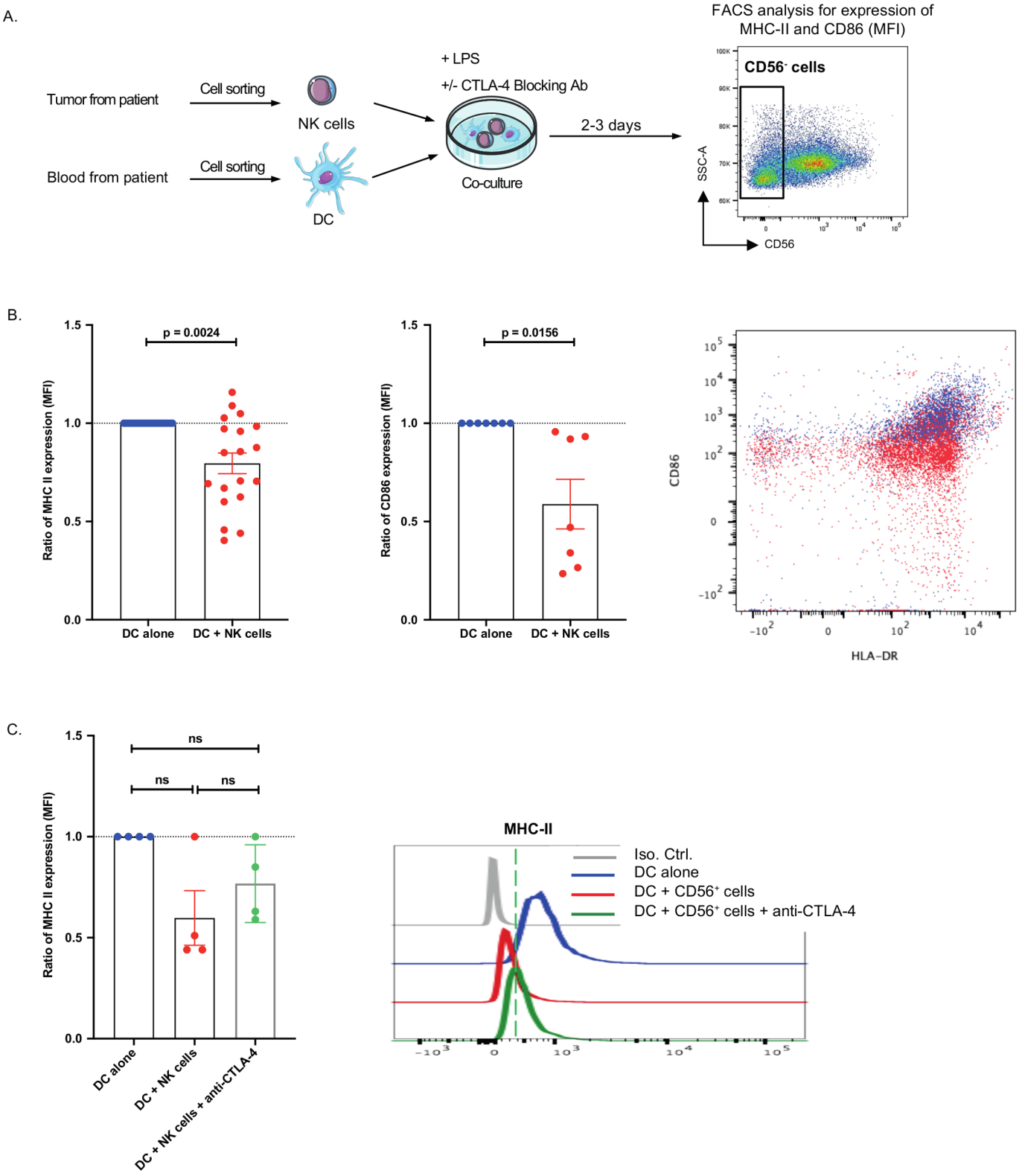

Figure 5 Intratumoral natural killer (NK) cells reduces dendritic cell (DC) maturation. (A,B) major histocompatibility complex (MHC)-II and CD86 surface expression was analyzed by flow cytometry on lipopolysaccharide (LPS)-treated CD11c$^+$ DC after 2–3 days of co-culture with CD3$^-$CD56$^+$ intratumoral NK cells. Experimental design of the co-culture experiment is shown in (A). (B) Expression of CD86 or MHC-II expression on LPS-treated DC alone (DC alone) or in co-culture with CD56$^+$ cells (DC +CD56$^+$ cells) was analyzed. Data are represented as a ratio of mean fluorescence intensity of CD86 or MHC-II expression in DC alone (blue dots) versus DC +CD56$^+$ cells co-culture (red dots). (C) The ratio of MHC-II surface protein expression on LPS-treated DC were analyzed by flow cytometry after 3–4 days of culture of DC cells alone (blue dots) or in co-culture with CD56$^+$ cells (red dots) and in the presence of cytotoxic T-lymphocyte-associated protein 4 (CTLA4) blocking antibody (green triangles). Statistical analyses were performed by the Wilcoxon non-parametric test with the GraphPad software. ns: not significant.

J Immunother Cancer: first published as 10.1136/jitc-2020-001054 on 16 October 2020. Downloaded from http://jitc.bmj.com/ on February 6, 2023 at INSERM Consortia. Protected by copyright.

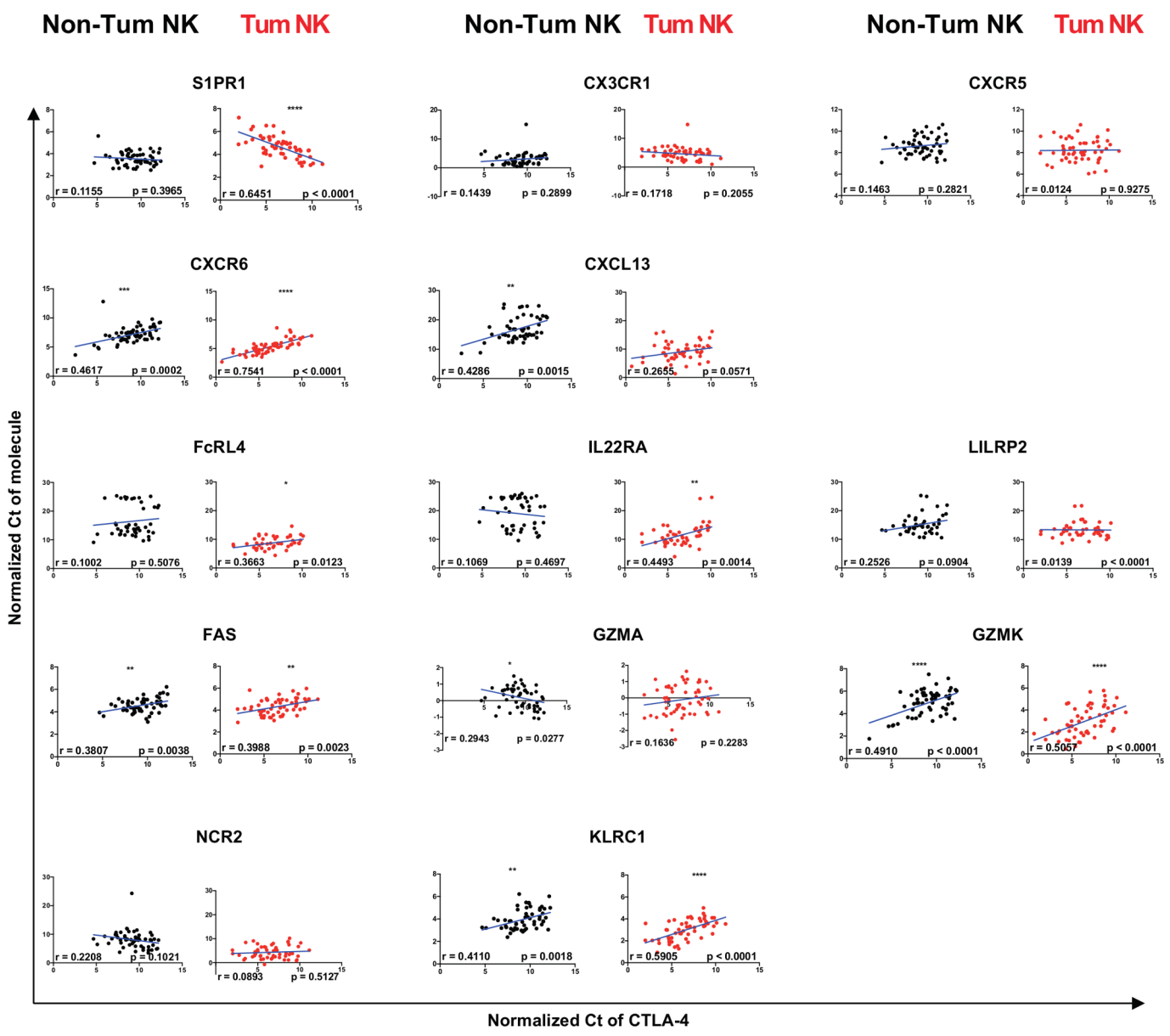

Figure 6 Correlation between cytotoxic T-lymphocyte-associated protein 4 (CTLA4) expression and gene signature expression in tumor versus non-tumorous NK cells Sorted NK cells from non-tumorous distant tissue (Non-Tum NK) and tumorous (Tum NK) for 47 patients were extracted and total RNA was analyzed. CTLA4 mRNA expression was then compared with Ct values of the 14 genes previously identified. The correlation between both values was assessed in non-tumorous and tumorous NK cells using Pearson correlation test with the GraphPad software.

CXCR6, GZMK and KLRC1, an inhibitory receptor on NK cells (figure 6). This suggests that CTLA4-expressing NK subsets may have a distinct migration and regulatory function profiles as compared with other NK cells.

Intratumoral NK cells negatively impact the clinical outcome of CD8$^+$ T cells

To investigate whether the presence of intratumoral NK cells could impact the clinical outcome, the localization and density of tumor-infiltrating NK cells were determined by NKp46 quantification on a retrospective cohort of patients with NSCLC.[27] Immunohistochemistry (IHC) staining revealed that NKp46$^+$ cells were mainly localized in the stroma and poorly infiltrated the tumor nest (see online supplemental figure S6).

The prognostic value of intratumoral NK cells was determined using median cut-off separation of the groups. NK cell density was not linked to a prognosis in the entire cohort (figure 7A), in stages I and II (see online supplemental figure S7A), tumor size (see online supplemental figure S7B), histological subgroups (see online supplemental figure S7C) or chronic obstructive pulmonary disease (COPD) patients (see online supplemental figure S7D). Since some subsets of NK cells express inhibitory markers, including KLRC1 and CTLA4, we hypothesized that the presence of inhibitory NK cells could impact on

J Immunother Cancer: first published as 10.1136/jitc-2020-001054 on 16 October 2020. Downloaded from http://jitc.bmj.com/ on February 6, 2023 at INSERM Consortia. Protected by copyright.

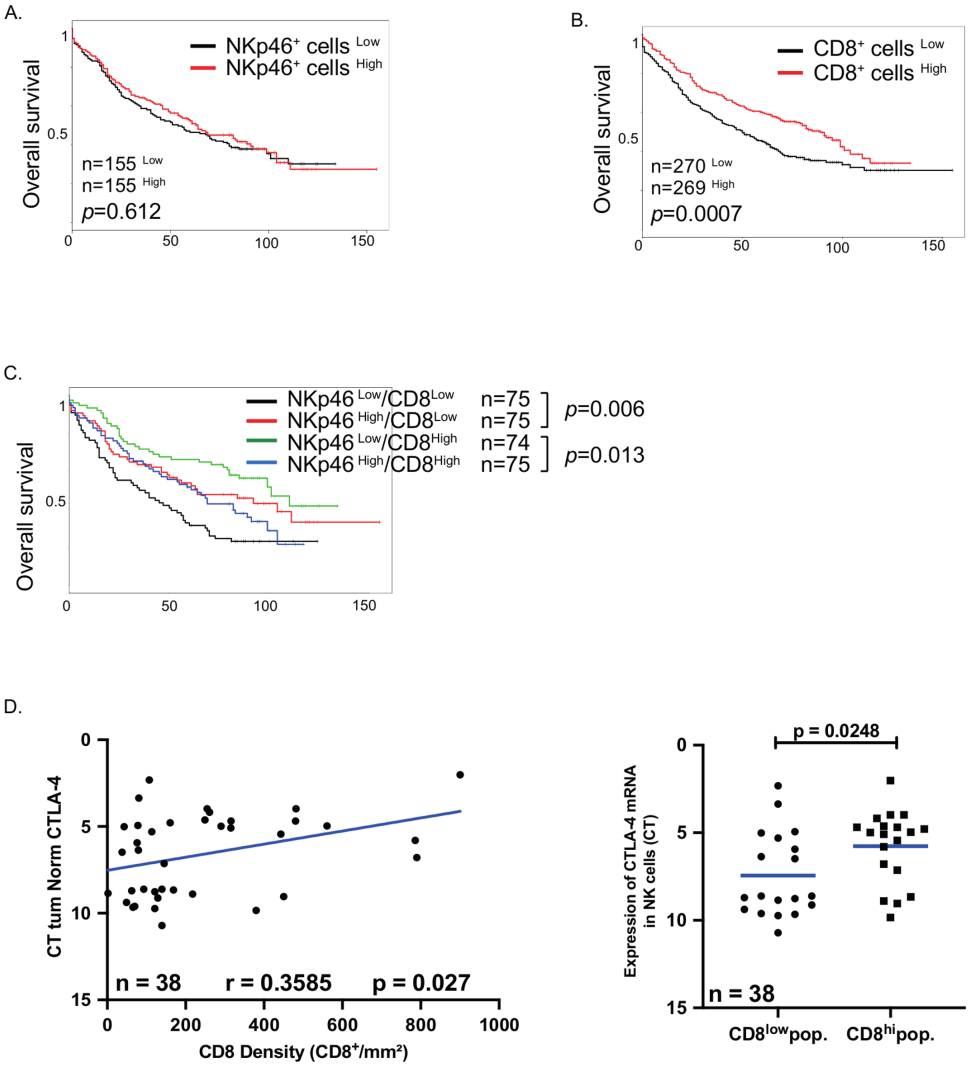

Figure 7 Clinical impact of NKp46$^+$ cells in patients with non-small cell lung carcinoma. (A,B) Patients from the retrospective cohort (cohort 3) were splitted into two groups according to the density of intratumoral NKp46$^+$ cells (A) or CD8$^+$ cells (B). Separation was done by median and their overall survival was analyzed. (C) Patients with low density (CD8$^+$ cells^{Low}) or high density (CD8$^+$ cells^{High}) of CD8$^+$ cells were splitted into two groups according to their number of intratumoral Nkp46$^+$ cells and the overall survival were done in each group. Separation was done by median. (D,E) CD8 density of patients from the validation cohort (cohort 2) was assessed by immunohistochemistry on paraffin-embedded slides and the correlation with cytotoxic T-lymphocyte-associated protein 4 (CTLA4) mRNA expression in natural killer (NK) cells was calculated using Pearson correlation test with the GraphPad software (D). (E) Patients from validation cohort (cohort 2) were split in two groups according to the density of intratumoral CD8$^+$ cells (using median) and the expression of CTLA4 mRNA was analyzed in each group. Statistical analyses were performed by the Mann-Whitney non-parametric test with the GraphPad software.

the prognostic value of CD8$^+$ T cells. As previously reported, high CD8$^+$ T cell density strongly correlated to a good clinical outcome[14] (figure 7B). Consequently, the prognostic impact of NK cells differed when considering patient groups with high or low CD8$^+$ T cell infiltration. In patients with low numbers of CD8$^+$ T cells, high NK cell density improved the clinical outcome, whereas in patients with high CD8$^+$ T cell density, NK cells negatively impacted the OS (figure 7C), supporting the inhibitory role of intratumoral NK cells. This prognostic effect of NK cells is specific of T cells, since NK cell densities did not impact the clinical impact of B cells and mature DC-LAMP$^+$ DCs (see online supplemental figure S8).

CTLA4 expression by intratumoral NK cells is correlated to CD8$^+$ T cell density

Considering the expression pattern and suppressive role of CTLA4 in tumor NK cells, we investigated the dynamics of CTLA4 in tumor NK cells in the prospective cohort described in table 2 (cohort 2). We found a positive correlation between the density of CD8$^+$ T cells and the level of CTLA4 gene expression by intratumoral NK cells (figure 7D), and a positive correlation between the percentage of CTLA4$^+$ NK cells and the total percentage of CD3$^+$ T cells (see online supplemental figure S9A). Finally, we also found a positive correlation between the gene expression level of CTLA4 and CD4 or CD8,

J Immunother Cancer: first published as 10.1136/jitc-2020-001054 on 16 October 2020. Downloaded from http://jitc.bmj.com/ on February 6, 2023 at INSERM Consortia. Protected by copyright.

both in ADC and SCC (see online supplemental figure S9B), using gene expression profiling interactive analysis tool (http://gepia2.cancer.pku.cn/). Of note, total NK cell densities did not correlate with numbers of $CD8^+$ T cells, B cells or DCs (see online supplemental table S5), suggesting that the possible inhibitory effect of NK cells was restricted to the subset of CTLA4 expressing NK cells.

DISCUSSION

In previous studies, we found that intratumoral NK cells exhibit altered phenotypes and functions[7] characterized by a specific gene expression signature.[26] Here, we extended this study with an in-depth transcriptomic analysis of NK cells in human NSCLC comparing the signature of intratumoral NK cells with distant non-tumorous lung NK cells. Our results show a distinct transcriptomic signature of NK cells in the lung TME suggesting that the lung TME may induce suppressive NK cells, that could play a role in the regulation of antitumor adaptive immunity.

Our signature is enriched with the chemokine receptors CXCR5, CXCR6 and a show a strong downregulation of S1PR1 and CX3CR1. The density of NK cells in the TME is lower than in distant tissue[7] and NK cells in the TME express more CXCR6 and less CX3CR1. This specific migratory signature could explain the exclusion of NK cells from the tumor core. Indeed, several studies show the involvement of CX3CR1 and fractalkine—the latter being expressed by tumor cells—in the recruitment and cytotoxicity of NK cells against tumors,[31] and have shown TGF-β-mediated downregulation of CX3CR1.[32] In addition, CX3CR1-deficient mice have a defective antitumor response.[33] On the other hand, a population of NK cells expressing CXCR6 is characterized by a more immature phenotype, producing fewer cytotoxic mediators and proinflammatory cytokines.[34] The mechanism that explain this migratory profile found in intratumoral NK cells is unknown, but could be due to a preferential migration of cells that display this specific signature, to a local modification induced by the TME or a combination of both.

Intratumoral NK cells are also enriched with a number of inhibitory receptors most notable of which is CTLA4, a well-known immune checkpoint molecule expressed by effector T cells after TCR activation. It regulates T-cell activation by out-competing the co-stimulatory molecule CD28 by binding its partners CD80 and CD86 with a higher avidity.[30] However, data on the expression and function of CTLA4 in NK cells are scarce and poorly investigated. In studies by Chiossone *et al*[35] and Terme *et al*,[36] CTLA4 transcripts were detected by whole-genome microarray analysis of mouse NK cells, indicating that CTLA4 may be expressed by NK cells. In a recent study, CTLA4 was found in $CD69^+CD103^+$ tissue resident NK cell subsets in human lungs,[37] and CTLA4 expression is shown to be upregulated in activated murine[38] and human[39] NK cells. However, there is no evidence demonstrating CTLA4 expression by NK cells in the context of human lung tumors. We found that a subpopulation of intratumoral NK cells have intracellular CTLA4, as previously observed in a murine model of lung tumors, showing CTLA4 gene expression by intratumoral NK cells.[38] Our immunohistochemistry studies reveal that CTLA4 is co-expressed with NKp46 also in other solid tumors suggesting that its expression by NK cells is not restricted to lung tumors. Several isoforms of CTLA4 have been characterized.[40] By RT-PCR, we found all the isoforms in NK cells purified from NSCLC tumors (data not shown). Interestingly, CTLA4 expression strongly correlated with that of another inhibitory receptor KLRC1, specifically in the tumor tissue and co-expression of both inhibitory receptors was confirmed in intratumoral NK cells, suggesting that, in the TME, NK cells acquire inhibitory receptors making them less efficient effector cells.

The mechanism of action of CTLA4 is still not completely clear. In co-culture experiments, we found that tumor NK cells reduced DC maturation, and this was partially reversed by the addition of CTLA4 blocking antibodies. A possible effect of secreted CTLA4 was excluded since we did not detect soluble CTLA4 in the NK cell supernatants. The precise mechanism of this inhibition is unclear, but it could involve CTLA4 -by maintaining its expression at the surface level in the presence of the anti CTLA4 Ab, as it has been suggested[41]—and other yet unidentified molecules secreted or expressed by tumor-experienced NK cells, blocking the maturation or the recruitment of DC. Indeed, instances of NK cells suppressive DCs have been reported in previous studies: upregulation of PD-L1 on NK cells and PD-1 on DC led to impaired DC maturation and low $CD8^+$ T cell priming,[42] while the impaired NK cell viability caused by tumor released prostaglandin E2 led to reduced recruitment of cDC1 in the TME.[43]

While intratumoral NK cells exhibit altered functions, their density within the TME does not associate with improved clinical outcome, contrary to $CD8^+$ T cells that are linked to good OS. Surprisingly, we found that high density of NK cells associates with a good OS only in patients with low infiltration of $CD8^+$ cells, whereas it conferred a poor outcome in patients with high CD8 density. This highlights a role for the tumor immune microenvironment in reprogramming NK cells. Accordingly, we found a positive correlation between higher $CD8^+$ T cell infiltration with CTLA4 expression by NK cells suggesting that immune-active tumors also harbor suppressive NK cells. Of note, high NK cells density was also linked to good clinical outcome in COPD patients.[27]

Despite the fact that NK cells have been widely implicated in antitumorous immune responses in various tumor models, several studies highlight their potential inhibitory/regulatory role. Regulatory NK cells produce IL-10 and/or express the immune checkpoint molecule CD73 and inhibit autologous $CD4^+$ T cell proliferation.[21 44 45] Activated NK cells express granzyme K and NCR2[46 47] and kill autologous activated $CD4^+$ T cells by a mechanism involving granzyme K.[48] We found that NK cells from the TME have a phenotype of activated

J Immunother Cancer: first published as 10.1136/jitc-2020-001054 on 16 October 2020. Downloaded from http://jitc.bmj.com/ on February 6, 2023 at INSERM Consortia. Protected by copyright.

cells—expressing CD69 and NCR2 molecules—and we found a strong correlation between CTLA4 and GZMK expression, suggesting that tumor-experienced CTLA4$^+$ NK cells could kill CD4$^+$ T cells. However, we did not find any decrease in T cell populations in tumors enriched in CTLA4$^+$ NK cells. The inhibitory function of intratumoral NK cells was also reported by Crome *et al*,[49] who defined in high grade serous ovarian tumors a population of regulatory CD56$^+$CD3$^-$ cells that suppressed TIL expansion, displayed low cytotoxic activity and produced IL-9 and IL-22 cytokines. This population resembles partially the one we describe in our study, based on cytokine profile and phenotypic characteristics. Finally, in advanced NSCLC, a regulatory role of NKp46 +NK cells has been reported, showing that low rates of circulating NKp46$^+$ NK cells significantly associated with better OS.[50]

CONCLUSIONS

Our findings on the regulatory function of NK cells in the lung TME have several therapeutic implications. First, the characterization of intratumoral NK cells reveals a specific migration profile potentially restricting their entry into the TME. It would be of great interest to target chemokine receptors on NK cells to enable them to enter tumor tissues. Second, our results show that NK cells acquire inhibitory functions within the TME, the reversion of which will enable NK cells to activate other immune cells and exert antitumorous cytotoxic functions. During the past 10 years, antibodies targeting CTLA4 and PD1/PD-L1 have entered clinical trials to reverse T cell exhaustion and restore the antitumor capacity of T cells, with proven efficacy in patients with various types of advanced cancers, including NSCLC.[51] In addition, several clinical trials based on NK cell checkpoints are ongoing, targeting KIR, TIGIT, lymphocyte-activation gene 3, TIM3 and KLRC1.[19] In this context, both CD8$^+$ T cells and NK cells have been shown necessary for the therapeutic effectiveness of combination IL-2 and CTLA4 blockade immunotherapy in B16 melanoma.[52] Our study provides data supporting the pertinence of targeting the inhibitory activity of NK cells within the TME.

In conclusion, our results support the notion that the TME contains regulatory NK cells that represents a new escape mechanism.

Author affiliations
[1]Centre de Recherche des Cordeliers, Sorbonne Universite, Inserm, Universite de Paris, Team Inflammation, complement and cancer, F-75006, Paris, France
[2]Programme Cartes d'Identité des Tumeurs, Ligue Nationale Contre le Cancer, Paris, France
[3]Universite de Paris. Laboratoire d'immunologie, Hopital Europeen Georges Pompidou, APHP, Paris, France
[4]Sorbonne Universite, INSERM U1135, Centre d'Immunologie et des Maladies Infectieuses, Team Immune Microenvironment and Immunotherapy, F-75013, Paris, France
[5]Department of Pathology, Institut Mutualiste Montsouris, Paris, France
[6]Departments of Pathology and Thoracic Surgery, Hospital Cochin Assistance Publique Hopitaux de Paris, F-75014, Paris, France
[7]INSERM U1015, Gustave Roussy, 114 rue Edouard Vaillant, 94805, Villejuif Cedex, France
[8]Universite Paris Saclay, Le Kremlin-Bicêtre, France
[9]Centre de Recherche des Cordeliers, Sorbonne Universite, Inserm, Universite de Paris, Team Laboratory of Integrative cancer immunology, F-75006, Paris, France

Present affiliations The present affiliation of Mélanie Gillard-Bocquet is: INSERM, U1212-ARNA, Institut Européen de Chimie et de Biologie, F-33607 Pessac, France; Claire Germain is: Invectys-Cancer Immunotherapeutics, Paris, France and Jérémy Goc is: Joan and Sanford I. Weill Department of Medicine, Division of Gastroenterology and Hepatology, Department of Microbiology and Immunology and The Jill Robert's Institute for Research in Inflammatory Bowel Disease, Weill Cornell Medicine, Cornell University, New York, United States.

Twitter Florent Petitprez @petitprez_f and Isabelle Cremer @CremerIsabelle

Acknowledgements We thank the Cochin hospital for contributing to the tissue collection. We also thank the CHIC (Center of Histology Imaging and Cytometry) facility of the Centre de Recherche des Cordeliers.

Contributors PEJ, JR, MGB, CT, SM, NJ, CG, JG and MADD performed the experiments. MM, FP and GB performed bioinformatic analysis. PEJ, JR, CT, MGB and IC analyzed the data. PV, LF, AL, DD and MA provided clinical samples and pathological data. IC designed and supervised the study. PEJ, JR, MG-B and IC wrote the manuscript. AV, MCDN and LZ revised the manuscript.

Funding This work was supported by the 'Institut National de la Sante et de la Recherche Medicale', Sorbonne Universite, Universite de Paris, the LabEx Immuno-Oncology and the Institut National du Cancer (2017-PLBIO). JR was supported by Sorbonne Universite.

Competing interests None declared.

Patient consent for publication Not required.

Ethics approval All the patients gave an informed consent prior to inclusion. The study was conducted with the agreement of the French ethic committee (number 2012 06 12 IRB00001072) in application with the article L. 1121-1 of French law, according to the recommendations in the Declaration of Helsinki.

Provenance and peer review Not commissioned; externally peer reviewed.

Data availability statement Data are available upon reasonable request. Data availability will be possible from Isabelle Cremer.

Supplemental material This content has been supplied by the author(s). It has not been vetted by BMJ Publishing Group Limited (BMJ) and may not have been peer-reviewed. Any opinions or recommendations discussed are solely those of the author(s) and are not endorsed by BMJ. BMJ disclaims all liability and responsibility arising from any reliance placed on the content. Where the content includes any translated material, BMJ does not warrant the accuracy and reliability of the translations (including but not limited to local regulations, clinical guidelines, terminology, drug names and drug dosages), and is not responsible for any error and/or omissions arising from translation and adaptation or otherwise.

Open access This is an open access article distributed in accordance with the Creative Commons Attribution Non Commercial (CC BY-NC 4.0) license, which permits others to distribute, remix, adapt, build upon this work non-commercially, and license their derivative works on different terms, provided the original work is properly cited, appropriate credit is given, any changes made indicated, and the use is non-commercial. See http://creativecommons.org/licenses/by-nc/4.0/.

ORCID iD
Isabelle Cremer http://orcid.org/0000-0002-0963-1031

REFERENCES

1 Vivier E, Artis D, Colonna M, *et al*. Innate lymphoid cells: 10 years on. *Cell* 2018;174:1054–66.
2 Schmidt L, Eskiocak B, Kohn R, *et al*. Enhanced adaptive immune responses in lung adenocarcinoma through natural killer cell stimulation. *Proc Natl Acad Sci U S A* 2019;116:17460–9.
3 López-Soto A, Gonzalez S, Smyth MJ, *et al*. Control of metastasis by NK cells. *Cancer Cell* 2017;32:135–54.
4 Morvan MG, Lanier LL. NK cells and cancer: you can teach innate cells new tricks. *Nat Rev Cancer* 2016;16:7–19.
5 Villegas FR, Coca S, Villarrubia VG, *et al*. Prognostic significance of tumor infiltrating natural killer cells subset CD57 in patients with squamous cell lung cancer. *Lung Cancer* 2002;35:23–8.

J Immunother Cancer: first published as 10.1136/jitc-2020-001054 on 16 October 2020. Downloaded from http://jitc.bmj.com/ on February 6, 2023 at INSERM Consortia. Protected by copyright.

6 Carrega P, Morandi B, Costa R, *et al*. Natural killer cells infiltrating human nonsmall-cell lung cancer are enriched in CD56 bright CD16(-) cells and display an impaired capability to kill tumor cells. *Cancer* 2008;112:863–75.
7 Platonova S, Cherfils-Vicini J, Damotte D, *et al*. Profound coordinated alterations of intratumoral NK cell phenotype and function in lung carcinoma. *Cancer Res* 2011;71:5412–22.
8 Pasero C, Gravis G, Guerin M, *et al*. Inherent and tumor-driven immune tolerance in the prostate microenvironment impairs natural killer cell antitumor activity. *Cancer Res* 2016;76:2153–65.
9 Mamessier E, Sylvain A, Thibult M-L, *et al*. Human breast cancer cells enhance self tolerance by promoting evasion from NK cell antitumor immunity. *J Clin Invest* 2011;121:3609–22.
10 Zhang Q-F, Yin W-W, Xia Y, *et al*. Liver infiltrating CD11b CD27 NK subsets account for NK cell dysfunction in patients with hepatocellular carcinoma and are associated with tumor progression. *Cell Mol Immunol* 2017;14:819–29.
11 Rusakiewicz S, Semeraro M, Sarabi M, *et al*. Immune infiltrates are prognostic factors in localized gastrointestinal stromal tumors. *Cancer Res* 2013;73:3499–510.
12 Cong J, Wang X, Zheng X, *et al*. Dysfunction of natural killer cells by FBP1-Induced inhibition of glycolysis during lung cancer progression. *Cell Metab* 2018;28:243–55.
13 Dieu-Nosjean M-C, Antoine M, Danel C, *et al*. Long-term survival for patients with non-small-cell lung cancer with intratumoral lymphoid structures. *J Clin Oncol* 2008;26:4410–7.
14 Goc J, Germain C, Vo-Bourgais TKD, *et al*. Dendritic cells in tumor-associated tertiary lymphoid structures signal a Th1 cytotoxic immune contexture and license the positive prognostic value of infiltrating CD8+ T cells. *Cancer Res* 2014;74:705–15.
15 Germain C, Gnjatic S, Tamzalit F, *et al*. Presence of B cells in tertiary lymphoid structures is associated with a protective immunity in patients with lung cancer. *Am J Respir Crit Care Med* 2014;189:832–44.
16 Catacchio I, Scattone A, Silvestris N, *et al*. Immune Prophets of lung cancer: the prognostic and predictive landscape of cellular and molecular immune markers. *Transl Oncol* 2018;11:825–35.
17 Hervier B, Russick J, Cremer I, *et al*. NK cells in the human lungs. *Front Immunol* 2019;10:1263.
18 Lavin Y, Kobayashi S, Leader A, *et al*. Innate immune landscape in early lung adenocarcinoma by paired single-cell analyses. *Cell* 2017;169:750–65.
19 Sun H, Sun C. The rise of NK cell checkpoints as promising therapeutic targets in cancer immunotherapy. *Front Immunol* 2019;10:2354.
20 Muntasell A, Ochoa MC, Cordeiro L, *et al*. Targeting NK-cell checkpoints for cancer immunotherapy. *Curr Opin Immunol* 2017;45:73–81.
21 Neo SY, Yang Y, Record J, *et al*. CD73 immune checkpoint defines regulatory NK cells within the tumor microenvironment. *J Clin Invest* 2020;130:1185–98.
22 Delconte RB, Kolesnik TB, Dagley LF, *et al*. CIS is a potent checkpoint in NK cell-mediated tumor immunity. *Nat Immunol* 2016;17:816–24.
23 André P, Denis C, Soulas C, *et al*. Anti-NKG2A mAb is a checkpoint inhibitor that promotes anti-tumor immunity by Unleashing both T and NK cells. *Cell* 2018;175:1731–43.
24 Zhang Q, Bi J, Zheng X, *et al*. Blockade of the checkpoint receptor TIGIT prevents NK cell exhaustion and elicits potent anti-tumor immunity. *Nat Immunol* 2018;19:723–32.
25 Chiossone L, Dumas P-Y, Vienne M, *et al*. Natural killer cells and other innate lymphoid cells in cancer. *Nat Rev Immunol* 2018;18:671–88.
26 Gillard-Bocquet M, Caer C, Cagnard N, *et al*. Lung tumor microenvironment induces specific gene expression signature in intratumoral NK cells. *Front Immunol* 2013;4:19.
27 Biton J, Ouakrim H, Dechartres A, *et al*. Impaired tumor-infiltrating T cells in patients with chronic obstructive pulmonary disease impact lung cancer response to PD-1 blockade. *Am J Respir Crit Care Med* 2018;198:928–40.
28 Bindea G, Mlecnik B, Hackl H, *et al*. ClueGO: a Cytoscape plug-in to decipher functionally grouped gene ontology and pathway annotation networks. *Bioinformatics* 2009;25:1091–3.
29 Shannon P, Markiel A, Ozier O, *et al*. Cytoscape: a software environment for integrated models of biomolecular interaction networks. *Genome Res* 2003;13:2498–504.
30 Rowshanravan B, Halliday N, Sansom DM. CTLA-4: a moving target in immunotherapy. *Blood* 2018;131:58–67.
31 Lavergne E, Combadière B, Bonduelle O, *et al*. Fractalkine mediates natural killer-dependent antitumor responses in vivo. *Cancer Res* 2003;63:7468–74.
32 Castriconi R, Dondero A, Bellora F, *et al*. Neuroblastoma-Derived TGF-β1 modulates the chemokine receptor repertoire of human resting NK cells. *J Immunol* 2013;190:5321–8.
33 Yu Y-RA, Fong AM, Combadiere C, *et al*. Defective antitumor responses in CX3CR1-deficient mice. *Int J Cancer* 2007;121:316–22.
34 Stegmann KA, Robertson F, Hansi N, *et al*. CXCR6 marks a novel subset of T-betloEomeshi natural killer cells residing in human liver. *Sci Rep* 2016;6:26157.
35 Chiossone L, Chaix J, Fuseri N, *et al*. Maturation of mouse NK cells is a 4-stage developmental program. *Blood* 2009;113:5488–96.
36 Terme M, Ullrich E, Aymeric L, *et al*. Cancer-induced immunosuppression: IL-18-elicited immunoablative NK cells. *Cancer Res* 2012;72:2757–67.
37 Marquardt N, Kekäläinen E, Chen P, *et al*. Unique transcriptional and protein-expression signature in human lung tissue-resident NK cells. *Nat Commun* 2019;10:3841.
38 Stojanovic A, Fiegler N, Brunner-Weinzierl M, *et al*. CTLA-4 is expressed by activated mouse NK cells and inhibits NK cell IFN-γ production in response to mature dendritic cells. *J Immunol* 2014;192:4184–91.
39 Lougaris V, Tabellini G, Baronio M, *et al*. CTLA-4 regulates human natural killer cell effector functions. *Clin Immunol* 2018;194:43–5.
40 Ward FJ, Dahal LN, Khanolkar RC, *et al*. Targeting the alternatively spliced soluble isoform of CTLA-4: prospects for immunotherapy? *Immunotherapy* 2014;6:1073–84.
41 Walker LSK, Sansom DM. Confusing signals: recent progress in CTLA-4 biology. *Trends Immunol* 2015;36:63–70.
42 Iraolagoitia XLR, Spallanzani RG, Torres NI, *et al*. NK cells restrain spontaneous antitumor CD8 T cell priming through PD-1/PD-L1 interactions with dendritic cells. *J Immunol* 2016;197:953–61.
43 Böttcher JP, Bonavita E, Chakravarty P, *et al*. NK cells stimulate recruitment of cdc1 into the tumor microenvironment promoting cancer immune control. *Cell* 2018;172:1022–37.
44 Morandi F, Horenstein AL, Chillemi A, *et al*. CD56brightCD16 – NK cells produce adenosine through a CD38-mediated pathway and act as regulatory cells inhibiting autologous CD4+ T cell proliferation. *J Immunol* 2015;195:965–72.
45 Vivier E, Ugolini S. Regulatory natural killer cells: new players in the IL-10 anti-inflammatory response. *Cell Host Microbe* 2009;6:493–5.
46 Bade B, Boettcher HE, Lohrmann J, *et al*. Differential expression of the granzymes A, K and M and perforin in human peripheral blood lymphocytes. *Int Immunol* 2005;17:1419–28.
47 Bratke K, Kuepper M, Bade B, *et al*. Differential expression of human granzymes A, B, and K in natural killer cells and during CD8+ T cell differentiation in peripheral blood. *Eur J Immunol* 2005;35:2608–16.
48 Jiang W, Chai NR, Maric D, *et al*. Unexpected role for granzyme K in CD56bright NK cell-mediated immunoregulation of multiple sclerosis. *J Immunol* 2011;187:781–90.
49 Crome SQ, Nguyen LT, Lopez-Verges S, *et al*. A distinct innate lymphoid cell population regulates tumor-associated T cells. *Nat Med* 2017;23:368–75.
50 Picard E, Godet Y, Laheurte C, *et al*. Circulating NKp46 Natural Killer cells have a potential regulatory property and predict distinct survival in Non-Small Cell Lung Cancer. *Oncoimmunology* 2019;8:e1527498.
51 Topalian SL, Hodi FS, Brahmer JR, *et al*. Safety, activity, and immune correlates of anti-PD-1 antibody in cancer. *N Engl J Med* 2012;366:2443–54.
52 Kohlhapp FJ, Broucek JR, Hughes T, *et al*. NK cells and CD8+ T cells cooperate to improve therapeutic responses in melanoma treated with interleukin-2 (IL-2) and CTLA-4 blockade. *J Immunother Cancer* 2015;3:18.

J Immunother Cancer: first published as 10.1136/jitc-2020-001054 on 16 October 2020. Downloaded from http://jitc.bmj.com/ on February 6, 2023 at INSERM Consortia. Protected by copyright.